MRS Communications (2023) 13:674–684

https://doi.org/10.1557/s43579-023-00412-8

MRS Communications

MRS 50th Anniversary Prospective

Synthesis and assembly of two-dimensional heterostructured architectures

Paraskevi Flouda, Jinyoung Choi, and Madeline L. Buxton, School of Materials Science and Engineering, Georgia Institute of Technology, Atlanta, GA 30332, USA
Dhriti Nepal, Materials and Manufacturing Directorate, Air Force Research Laboratory, Wright-Patterson Air Force Base, OH 45433, USA
Zhiqun Lin, School of Materials Science and Engineering, Georgia Institute of Technology, Atlanta, GA 30332, USA; Department of Chemical and Biomolecular Engineering, National University of Singapore, Singapore 117585, Singapore
Timothy J. Bunning, Materials and Manufacturing Directorate, Air Force Research Laboratory, Wright-Patterson Air Force Base, OH 45433, USA
Vladimir V. Tsukruk, School of Materials Science and Engineering, Georgia Institute of Technology, Atlanta, GA 30332, USA

Address all correspondence to Vladimir V. Tsukruk at **vladimir@mse.gatech.edu**

(Received 4 May 2023; accepted 27 July 2023; published online: 7 August 2023)

Abstract

Stacking atomically thin two-dimensional nanosheet materials leads to unique synergy in their inherent properties due to an intimate combination and matching that is not possible via separate individual components and phases. However, traditional synthesis and assembly methods result in poor architectural control, diffuse interfaces and restricted surface chemistry, thereby limiting their prospective potentials. This brief overview provides condensed consideration of different synthesis and assembly methods for the fabrication of diverse novel heterostructures from individual nanosheets and challenges of existing methods. Finally, future perspectives regarding crafting of well-defined heterostructures with highly controllable architectures and interfacial/surface chemistry and advanced characterization methods are highlighted.

Introduction

Two-dimensional (2D) nanomaterials, such as graphene, metal oxides (MO_xs), transition metal dichalcogenides (TMDs) and MXenes, have emerged as promising candidates for a wide variety of applications including sensing, flexible electronics and energy storage.[1] Among them, graphene and its derivatives are the most popular and widely reported for the past two decades (Fig. 1). As known, graphene, a single one-atom thick layer of sp^2-hybridized carbon atoms arranged in a hexagonal honeycomb lattice, possesses high surface area (~2630 m^2/g), conductivity (~10^6 S/cm), and Young's modulus (E~1.1 TPa).[2,3] It can be synthesized by both top-down and bottom–up methods.[2] The top-down methods include the *in-situ* exfoliation of graphite oxide, followed by reduction.[2] The bottom-up approaches include the production of graphene from precursors. Due to its exceptional properties, graphene and its derivatives have been exploited in diverse applications including energy storage and sensing.[2]

Metal oxides based on V_2O_5, SnO_2 or NiO are another class of functionalized 2D nanomaterials that has garnered increasing interest due to their ability to form ordered stacking morphologies, good electrochemical stability and high ionic conductivity.[10–14] 2D materials with an abundant gallery of controlled gap spacing and chemistry can not only promote the transfer of diverse ions for high reaction kinetics, but also provide new mechanisms and pathways for transport.[15,16] However, these materials often suffer from brittleness, hypersensitivity to moisture and oxygen and large charge-transfer resistance at interfaces.[17]

A rapidly emerging class of 2D nanomaterials is MXenes. These materials represent a large family of 2D transition metal carbides, nitrides, and carbonitrides with a general formula of $M_{n+1}X_nT_x$, where M is a transition metal, X is carbon and/or nitrogen, and T_x is the surface functional group (e.g., –OH, –O or –F), and n = 1, 2 or 3 (Fig. 1).[18–22] As known, MXenes are typically derived by the selective removal of the A-layer atoms (e.g., Si, Al, Ga) of a MAX phase through wet chemical or molten salt etching.[20–22] Benefiting from the high electronic conductivity, large specific surface area, and structural stability of MXenes, they can act as functional substrates for supporting nanocrystals of active materials (e.g., MO_x, where M = Mn, Fe, Co, Ni, Cu) for energy storage applications, energy storage, sensors, and electromagnetic interference (EMI) shielding.[4,23]

Nanomaterials, such as the graphene derivatives and MXenes discussed above, are potential ion/proton host and transport materials. To improve specific capacity and stability with controlled ion transport, one approach is to physically stack van der Waals heterostructures from different 2D materials in hetero-layered architectures (Fig. 1).[24] Individual nanosheets can be combined in diverse heterostructures by alternating dissimilar layers. As suggested, van der Waals forces can contribute to the stability of heterostructures with high binding energy.[25] For example, the combination of MXene and graphene sheets can provide synergistic metallic electrical conductivity of stacked layers.[26] Moreover, the structural similarity of MoS_2 and graphene provides a high possibility for correlated stacking.[7]

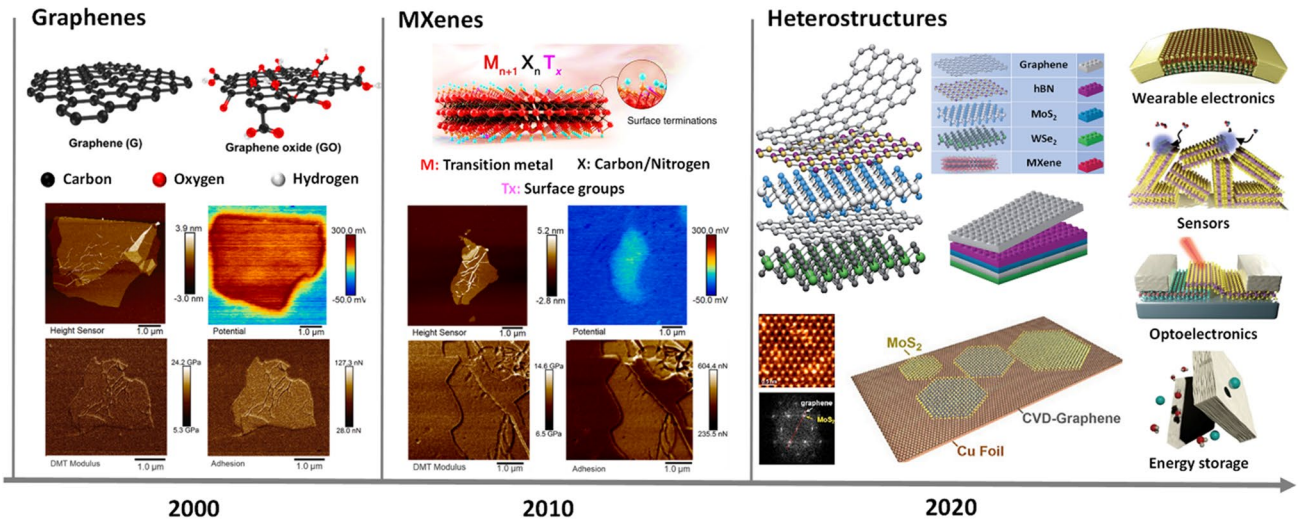

Figure 1. Overall timeline of the development of 2D nanomaterials including graphenes, MXenes and heterostructures. Combined from panels adapted with permission from Refs. 4–9.

Structural organization of 2D stacks greatly influences the conductivity and transport abilities with preferred domain orientation considered to be most efficient.[27,28] As demonstrated with poly(ethylene oxide) (PEO) based electrolytes, controlling the directional motion of ions is of great importance.[29–31] For example, highly ordered PEO oligomer-salt complexes could yield higher conductivity in the crystalline state due to organization of ion-conducting tunnels within the interlocking PEO chains.[29] In contrast to the conventional 'liquid-like' transport, the conduction mechanism was based on ion hopping along fixed pathways in a rigid lattice.[32] Vertical ordering of MXene/V_2O_5 heterostructures leads to significantly enhanced electron/ion transport over the lithium-ion battery electrodes compared to the horizontally ordered heterostructures due to shorter conduction pathways.[33]

The organization and interlayer spacing of 2D stacks can be controlled by the preparation conditions and interfacial chemistry (Fig. 2). For example, thinner graphene or MXene stacks will increase the specific surface area for incorporating more MO_x nanosheets to increase the energy density. Larger interlayer spacing of graphene or MXene can be explored for embedding MO_x nanosheets in the interspatial region of graphene or MXene for higher packing density, and thus may facilitate the enhanced intercalation of ions into heterostructures for higher ionic conductivity. Constructing higher order heterostructured materials with intercalated 2D materials (e.g., graphene oxides (GO), polyelectrolytes, and ionic liquids) with controlled interfacial bonding should be further considered. Furthermore, heterostacking and careful encapsulation may reduce oxidation, and prevent the excessive aggregation of MO_x nanosheets. However, a lack of deeper understanding regarding the fast transport mechanisms in hybrid nanocomposites, structured electrodes, and solid electrolytes hinders their practical use.[34–38]

To date, diverse 2D heterostructures (borophenes, silicenes, phosphorenes, graphenes and MXenes), have mainly been developed for lithium-ion batteries (LIBs).[39] For instance, 2D TMDCs-graphene (widely explored MoS_2-graphene, WS_2-graphene, SnS_2-graphene, and VS_2-graphene) have been reported as heterostructured electrodes for LIBs.[40] More recently, the use of 2D heterostructures has been investigated for zinc-ion and lithium-sulfur batteries, as well as for applications beyond energy storage such as EMI shielding and sensing.[41] For instance, MXene (V_2CT_x)/metal organic framework (MOF, Cu-HHTP) heterostructures were used as cathodes for zinc-ion batteries due to their enhanced structural stability and conductivity.[42] In another example, MXene/hexagonal boron nitride (h-BN) heterostructures have been investigated for EMI shielding performance.[43] Graphene/h-BN and cobalt oxide-functionalized MoS_2/graphene heterostructures were utilized as electrochemical biosensors for nicotine and glucose detection with detection limits of 0.4 μM and 30 nM, respectively.[44–46]

Despite the importance of ion and electron transport in confined 2D materials under electrical field in a number of fundamental processes, the key fundamental knowledge gap lies in the transport processes related to chemical modification of stacks. The direct monitoring of mobility and prevalence of carriers in confined and uniquely organized 2D heterostructures under electrical field have not been investigated thoroughly.[47] Shorter transport paths, low energy loss, interstacking gaps and electrokinetic energy losses at "turning points" have been discussed yet rarely investigated on a fundamental level for 2D heterostructures.

Here, we provide a brief overview of various ways to synthesize 2D heterostructures and highlight key scientific questions to be addressed in future studies, such as how the heterogeneous environment and induced surface chemistry of novel stacked nanostructures affect ion-wall chemical and physical interactions that can tailor ion diffusion under

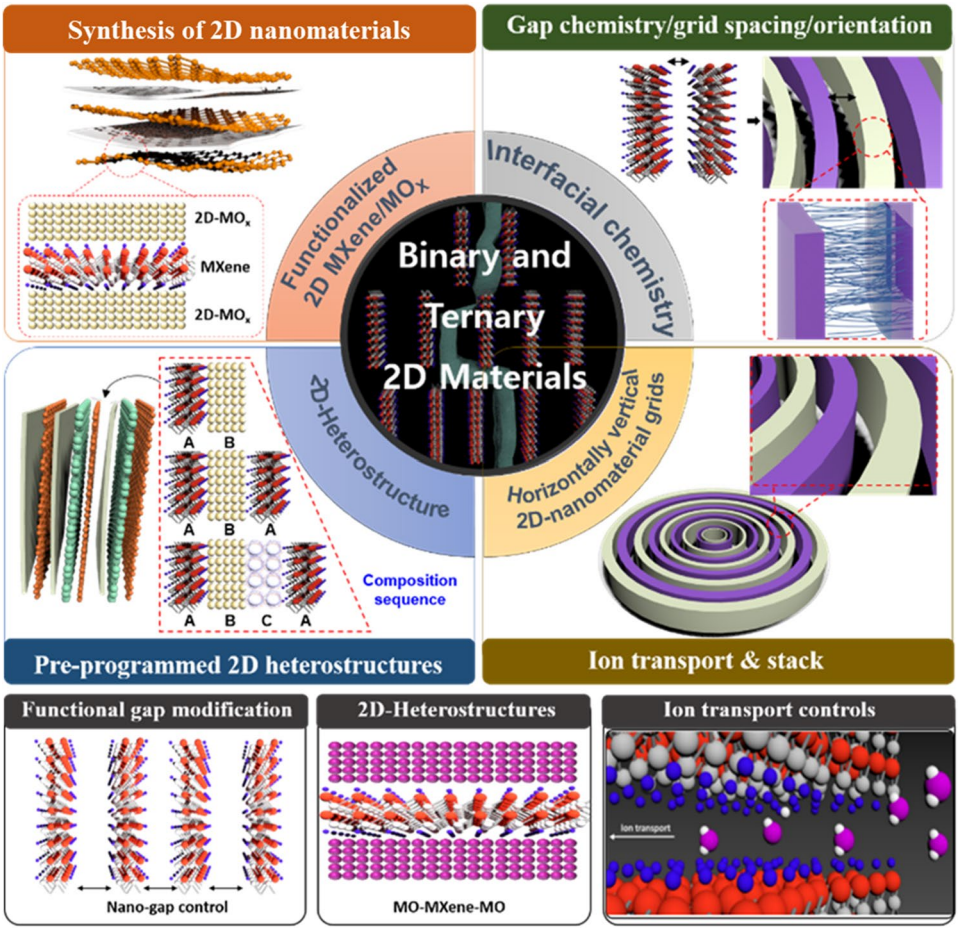

Figure 2. Summary of current and future efforts on synthesis and assembly of nanosheets and prospective 2D organized heterostructures with tailored surface chemistry, gap spacing, composition, morphology and properties.

confinement and may lead to fast ion transport. Our discussion will underline the rational design and synthesis of novel 2D MXene/MO_x heterostacked nanosheets through surface chemistry with direct synthetic approaches as supported by organized reactive templates. Finally, we discuss surface characterization methods to investigate the heterostructures and general trends in this field.

Fabrication of 2D heterostructures

To date, various approaches have been employed for the fabrication 2D heterostructures, such as self-assembly and *in-situ* growth methods including hydrothermal synthesis and chemical vapor deposition (CVD) (Fig. 3).[48,49] Among them, self-assembly is the most widely reported due to its versality. In contrast, *in-situ* growth methods are considered more challenging, yet can lead to a better control over surface chemistry, stacking manner and structures.[48,49]

Directed self-assembly

Self-assembly represents a popular route to the fabrication of 2D heterostructures that is based on tunable interfacial interactions between different nanomaterials, such as Coulombic and hydrogen bonding interactions, where precisely tunable physical properties can be achieved via controlling interaction strength of the two nanosheets. These methods have been investigated for a variety of different 2D heterostructures including MXene/V_2O_5, MXene/MOF, and MXene/MXene.[33,42,52]

Layer by layer (LbL) assembly is a well-established approach for the preparation of multilayered thin films with controlled thickness and composition by the alternating deposition of different layers.[53] The LbL technique has been used to develop heterostructured multilayers of various MXenes with amine functionalized reduced GO (rGO), polymers including polyethylene imine (PEI), poly(diallyldimethyl ammonium chloride) (PDADMA), and polyaniline, as well as positively charged amine functionalized $Ti_3C_2T_z$.[54–56] Such assemblies possess enhanced energy storage and sensing capabilities

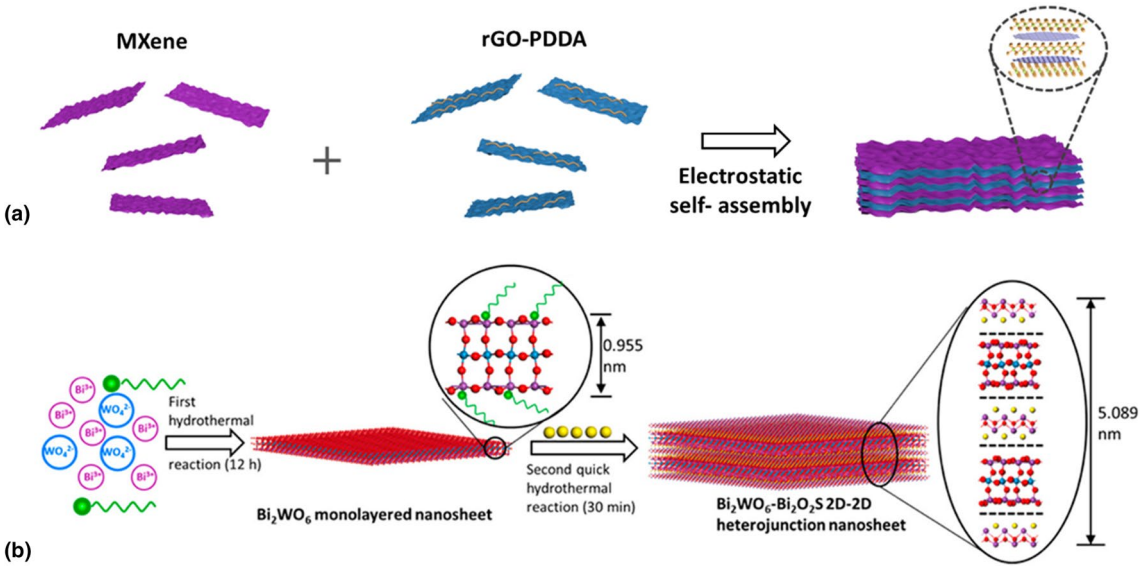

Figure 3. (a) Self-assembly of MXene and poly(diallyl dimethyl ammonium chloride) (PDDA) modified GO into heterostructures. (b) *In-situ* growth of Bi_2WO_6 and Bi_2O_2S 2D heterostructures using hydrothermal methods. Panels combined and adapted with permission from Refs. 50, 51.

resulting from the enhanced ion-conductivity.[54–56] Simple mixing of 2D nanosheets, followed by vacuum assisted filtration, cast drying, or freeze-drying is another well explored technique to create versatile heterostructures. For example, vertically aligned MXene/V_2O_5 were prepared by mixing MXenes with V_2O_5 sheets, followed by casting, freeze-drying, and compression.[33] Similarly, vertically pillared V_2CT_x/$Ti_3C_2T_x$ were prepared by vacuum filtration, leading to open ion-channels and mechanical stability.[52]

In-situ growth

In-situ growth methods are another widely studied group of approaches for the fabrication of the heterostructured stacks. The major advantages of the *in-situ* growth approaches include enhanced uniformity and stability, potentially enhanced ion transport between the stacks, and possibility to introduce binary and ternary super-heterostructures via tailored surface nanochemistry.[20,57]

Hydrothermal synthesis, a method based on the crystallization of a substance in aqueous media under high temperature and high vapor pressure conditions, is one of the major methods applied for *in-situ* growth. The combination of high pressure and heat allows for the synthesis of highly crystalline structures from precursors.[58] Several studies have shown that fine heterolayer structures comprised of metal oxides and 2D materials, including SnO_2/SnSe,[59] MoSe/MXene,[60] or MoS_2/MXene[61] have been synthesized through the hydrothermal synthesis and showed superior electrical performances through the enhanced mass transport between the layers. Another *in-situ* growth method is hydrolysis, which uses water to breakdown the covalent bonding and connect desired precursor material to the target surface. Through the method, multilayer Nb_2O_5 or V_2O_5 structures have been grown using rGO nanosheets or carbon nitride thin film as a template with high charge transfer property and high specific surface area.[62,63]

In-situ polymerization is another method with potential for the site-specific functionalization of the 2D structures. By using functionalized surface sites via electrostatic attraction, *in-situ* polymer growth can be directly conducted to grow additional polymer layers. Through this method, the combination of 2D structures with conductive polymers such MXene/polypyrrole and MXene/polyaniline have been reported to exhibit excellent electrical performance such as high capacitance and cycle durability.[64–66]

In addition, ALD and CVD, well-known techniques for the fabrication of high quality 2D materials and thin films, might be considered.[67] Involving the introduction of vaporized substance to the substrate to be decomposed or react with the substrate surface, the CVD process can yield uniform thin layer with larger area and multilayered superlattices such as SnS_2/WSe_2, and WSe_2/MoS_2/WSe_2.[63,68]

Future perspectives

Functionalized 2D heterostructures with controlled surface chemistry and programmed architectures can be instrumental for a variety of applications including energy storage, sensing and EMI shielding. However, the fabrication of diverse multilayers with strong, chemically bound interfaces between the layers remains a challenge, which also restricts the choice of the materials forming each layer. Furthermore, these limitations are intensified as the number of the layers and diversity of their nature increases. Advanced atomic force microscopy (AFM) characterization modes beyond conventional

topographic imaging, such as Kelvin probe force microscopy (KPFM), nano-DMA and AFM-IR, can offer insight in interfacial strengthening and physical heterostructure properties in addition to traditional high-resolution electron microscopies and X-ray relectivity.

Synthesis approaches

Further approaches for fabrication of different layered structures can be suggested to utilize the characteristics of strong-bonded, transport-friendly interlayers. As discussed above, carbon nitrides and graphene nanosheets have been used as templates for the synthesis of MO_xs, such as niobium pentoxide (Nb_2O_5) and vanadium pentoxide (V_2O_5).[62,69]

As known, MO_x nanosheets can be obtained via controlled hydrolysis of metal precursors by utilizing similar surface pendant groups and surface chemistry. During the synthesis process, the OH-pendant groups will not only provide the anchoring sites for precursors, but also serve as centers for condensation of metal oxy-trihydroxide formed during slow hydrolysis of metal precursors.[62,70] With the addition of a trace amount of water, fast hydrolysis can be achieved, yielding MO_x nanosheets.[62,69]

Next, expansion of the hydrolysis approach to different 2D templates, such as MXene nanosheets via its hydroxyl surface functional groups, can be explored. Figure 4(a) shows the potential use of MXene as a template by utilizing hydroxyl (–OH) and –F groups on their surfaces. The hydroxylic groups are capable of coordinating with transition metal precursors (e.g., niobium(V) ethoxide or vanadium oxytriisopropoxide (VOT)) over the surface of MXenes. Through subsequent hydrolysis, multilayer structures of Nb_2O_5 or V_2O_5 and MXene can be obtained.

A novel way of synthetizing multilayer heterostructures through combination of *in-situ* polymerization and previously reported block copolymer-based nanoreactors can be investigated to synthesize strong-bonded multilayer structure.[71] Specifically, growing appropriate block copolymers on the surface of the 2D nanosheets via surface-initiated atom transfer radical polymerization (SI-ATRP) can be utilized as a step toward synthesis of the nanoreactor template that can be used for further building of heterostructures.

Next, Fig. 4(b) illustrates the steps of the potential approach using MXene as a starting template. First, the surface hydroxyl (–OH) groups on MXene can be converted into bromide groups

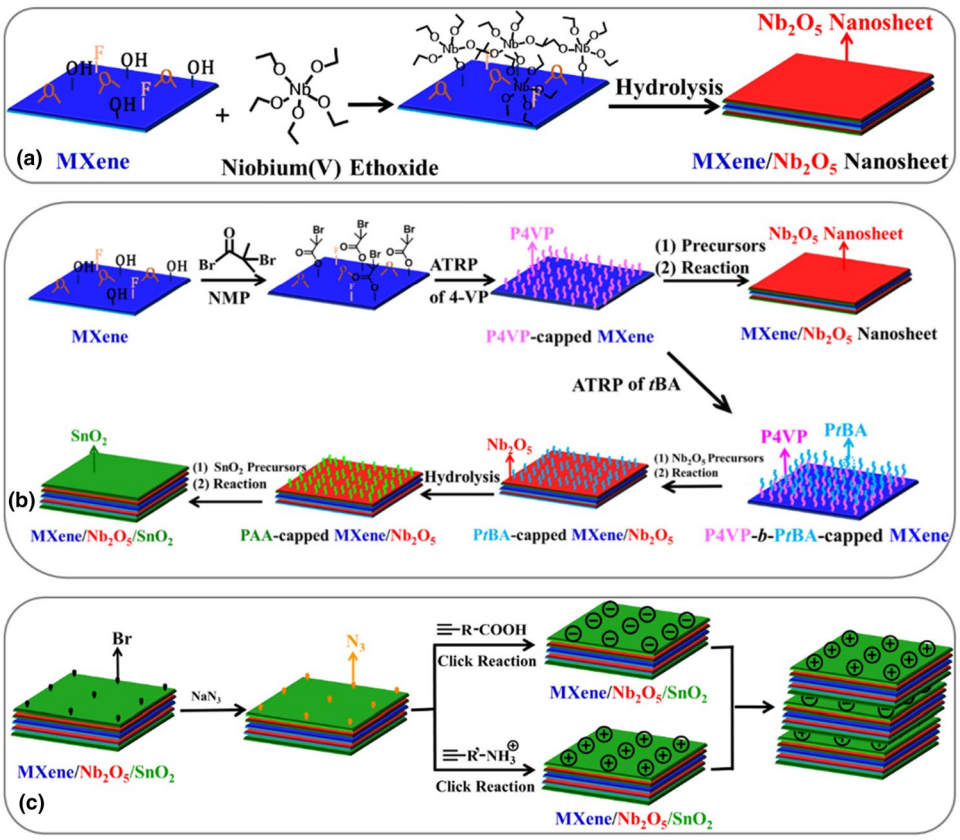

Figure 4. Suggested prospective *in-situ* growth of (a) Nb_2O_5 nanosheets on MXene surface templated by their functional groups (OH and O groups), (b) Nb_2O_5 or Nb_2O_5/SnO_2 nanosheets on MXene via surface-grafted poly(tert-butyl acrylate) (PtBA) or poly(4-vinylpyridine)-*block*-poly(acrylic acid) (P4VP-b-PAA) brushes as templates, respectively. (c) Synthesis of positively and negatively charged CBABC (A = MXene, B = Nb_2O_5, and C = SnO_2) stacks and their alternating layered assembly.

by reacting with 2-bromoisobutyl bromide, thereby forming bromide-terminated initiation surface sites for SI-ATRP. Second, poly(4-vinylprridine) (P4VP) can be grown by grafting from the MXene surface. The grown brush layer can be coordinated with metal precursors (e.g., niobium (V) ethoxide and VOT) to perform *in-situ* growth of MO_x nanocrystals as a follow-up step.

Furthermore, multilayer superstructures with a combination of different nanosheets can be achieved by using diblock copolymers composed of two different blocks. For example, a heterostructure of MXene/Nb_2O_5/SnO_2 can be grown in this manner. Specifically, amphiphilic di-block copolymer, poly(*tert*-butyl acrylate)-*block*-poly(4-vinylpyridine) (P*t*BA-*b*-P4VP), can be grafted on MXene surface via sequential SI-ATRP of 4-VP monomers in the first step, followed by *tert*-butyl acrylate (*t*BA) monomers, yielding a MXene-P4VP-PtBA template. Subsequently, Nb_2O_5 can be grown in the P4VP regime because of the coordination interaction between pyridyl groups of P4VP with metal precursors (i.e., niobium(V) ethoxide), resulting in P*t*BA-capped MXene/Nb_2O_5 nanosheets.

Thereafter, P*t*BA-capped MXene/Nb_2O_5 nanosheets can be transformed into PAA-capped MXene/Nb_2O_5 nanosheets using well-known hydrolysis procedure.[72] Finally, tin (IV) ethoxide precursors can be added and coordinated with the PAA blocks via the interaction between the carboxyl groups of PAA and metal moieties of precursors, yielding higher-level CBABC-type heterostructures with stacked MXene/Nb_2O_5/SnO_2 nanosheets (A = MXene, B = Nb_2O_5, and C = SnO_2).

In addition, these heterostructured stacks can be considered as a means for complementary long-term oxidation control during processing, storage, and utilization in order to retain properties of center layer (A), by complementary coverage of the facets. This approach is based upon known approaches in adding antioxidant species such as L-ascorbate or graphene oxide nanosheets to prevent the oxygen access to MXene surfaces.[73] Indeed, individual MXene flakes can be unstable in colloidal states due to oxidation of the titanium species. Some current methods for arresting oxidation include removal of oxygen from the solution by either inert gas purging or freezing the dispersions, or prohibiting contact with oxygen through dispersion of modified MXene in organic solvents.[74]

Moreover, the laminated heterostructured membranes can be formed through directed assembly of the pre-synthesized heterostructures. As has been demonstrated, TiO_2 nanorods, SnO_2 nanowires, graphene oxide, and Co_3O_4 nanoflakes can be assembled with $Ti_3C_2T_x$ MXene via the vacuum assisted filtration (VAF) driven by the interaction between the –OH groups on MO_xs and the –F groups on HF-etched $Ti_3C_2T_x$ MXene nanosheets.[75] Indeed, in a recent study, MXene and encapsulated MXene multilayer membranes have been successfully fabricated with the vacuum-assisted method.[76] We expect that by choosing processing conditions, ordered layered morphology can be extended across the whole membrane thickness with preserved orientation of 2D nanosheets over large surface areas.

As an alternative approach to create organized morphologies with alternating stacks, LbL assembly with complementary weak interactions can be further exploited.[53,77,78] Indeed, owing to the living characteristic of SI-ATRP, the end groups of polymer brushes (i.e., –Br) will remain exposed and can be converted into other functional groups [Fig. 4(c)]. For example, the –Br groups on the surface of MXene/Nb_2O_5/SnO_2 nanosheets can be converted into azide groups via reaction with NaN_3. Secondly, small molecules containing alkynyl and carboxyl groups at each end, respectively (≡–R′–COOH), can be grafted via click reaction under mild condition, yielding negatively-charged stacks. Meanwhile, the other small molecules containing alkynyl and quaternary ammonium groups (≡–R′–NH_3^+) can be grafted via click reaction, producing positively charged stacks. Then, alternating positively charged and negatively charged heterostructured stacks can be exploited to assemble via LbL technology, resulting in super-heterostructured materials. In addition, due to the introduction of diverse spacers (R and R′ groups of small molecules) the gap spacing can be tuned to tailor ion transport, storage, and interfacial chemistry of channels between alternating stacks.

Characterization

Comprehensive multi-length scale characterization of complex heterostructures and their physical properties is an extremely challenging task that requires the utilization of a battery of high-resolution spectroscopic and microscopic techniques. Beyond traditional electron microscopies, composition, interfaces, intercalation mechanisms and organization of hybrid stacked heterogeneous nanostructures can be probed with advanced electron microscopies and scanning probe imaging.[79]

For example, high-resolution selected area AFM in light tapping mode has been shown to clearly monitor over the reaction time a single structure, in this case a single MXene flake, enabling precise determination of the assembly of biopolymers and change in morphology and surface chemistry (Fig. 5).[76] To ensure the same MXene flake can be monitored during assembly process, pristine MXene flakes can be deposited on thermally oxidized silicon wafers with labeled grids for optical localization. The corresponding height histograms show the apparent flake thickness and a similar thickness before and after silk assembly promoted by complementary chemistry.

In another study, precise z-realignment of individual scan lines in high resolution image allowed to monitor real-time site-specific chemical reduction reaction on surface of the same 2D graphene nanosheet during chemical reduction with precision better than 0.1 nm in contrast to nominal accuracy of 0.2–0.3 nm (Fig. 6).[80] Concurrent monitoring of electrostatic forces renders observation of surface chemistry evolution during chemical reaction of hydrazine with nanoscale identification of site-specific diversity (Fig. 6). Such precise monitoring of assembly and surface chemistry evolution with atomic accuracy can be even more critical for novel heterostructured materials.

Friction anisotropy of heterostructures was shown by measuring lateral forces between asperities and surface of MXene flakes.[81] The anisotropic direction of the frictional force is highly dependent on thickness of the MXene layer.[81] Next, surface force spectroscopy (SFS) can provide precision and

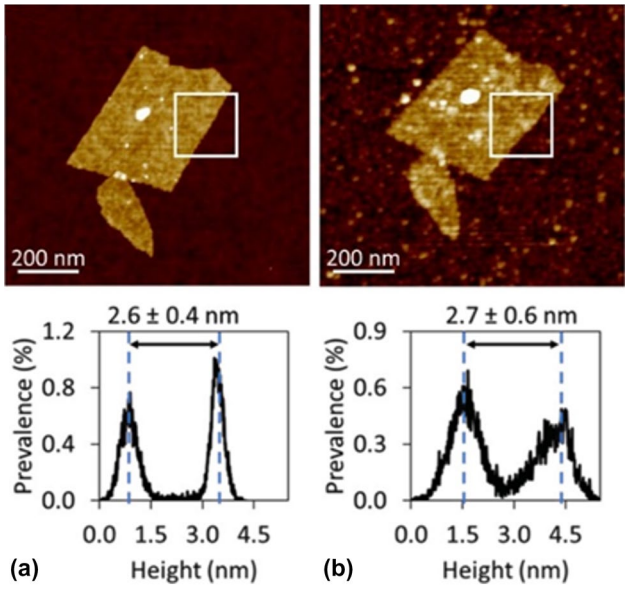

Figure 5. High resolution AFM images (top) of the same nanosheets before (a) and after (b) modification with silk fibroin of $Ti_3C_2T_x$ with square area selected for analysis of height histograms (bottom) for identification of nanoscale coating presence. Adapted with permission from Ref. 76.

localized measurements such as intermolecular interactions using force measurements of interaction between the AFM probe and the surfaces of heterostructured materials. Quantitative nanomechanical probing translates the force measured by tip-surface interaction into pull-off forces related to adhesion. Adhesive force measurements showed that varying precooling treatments can improve interfacial adhesion.[82,83] Another study showed how surface interactions are influenced by charge density of oxygen.[84] AFM imaging with power spectral density analysis of 2D materials on carbon fiber surfaces showed avenues for strengthening interfaces.[6]

Furthermore, surface electrical potential measurements with KPFM were applied to WSe_2–MoS_2 heterostructures (Fig. 7).[85] The researchers demonstrated spatial heterogeneity of individual heterostructures due to localized differences in the light-mediated resistive switching mechanism for sensing applications. Under UV illumination, *in-situ* potential differences observed their reduction over time due to increased light intensity of MXene and ZnO films as electron–hole pairs are generated at the interface of the heterostructure.[86]

Another intriguing AFM mode for in-depth nanoscale characterization of heterostructures is nano-IR.[87] This technique allows mapping of chemical composition of the heterostructures. Visualization of the spatial distribution at different frequencies shows local compositional and structural differences [Fig. 8(a–d)].[88]

Another instance of nano-IR mode is mapping of graphene surface plasmons formed on a pentacene, graphene heterostructure.[89] In this study, nano-IR has been used to show plasmon edge features around the distinct layers of the heterostructure which depend on the pentacene thickness and layer orientation. In related studies of polymer monolayers that can be

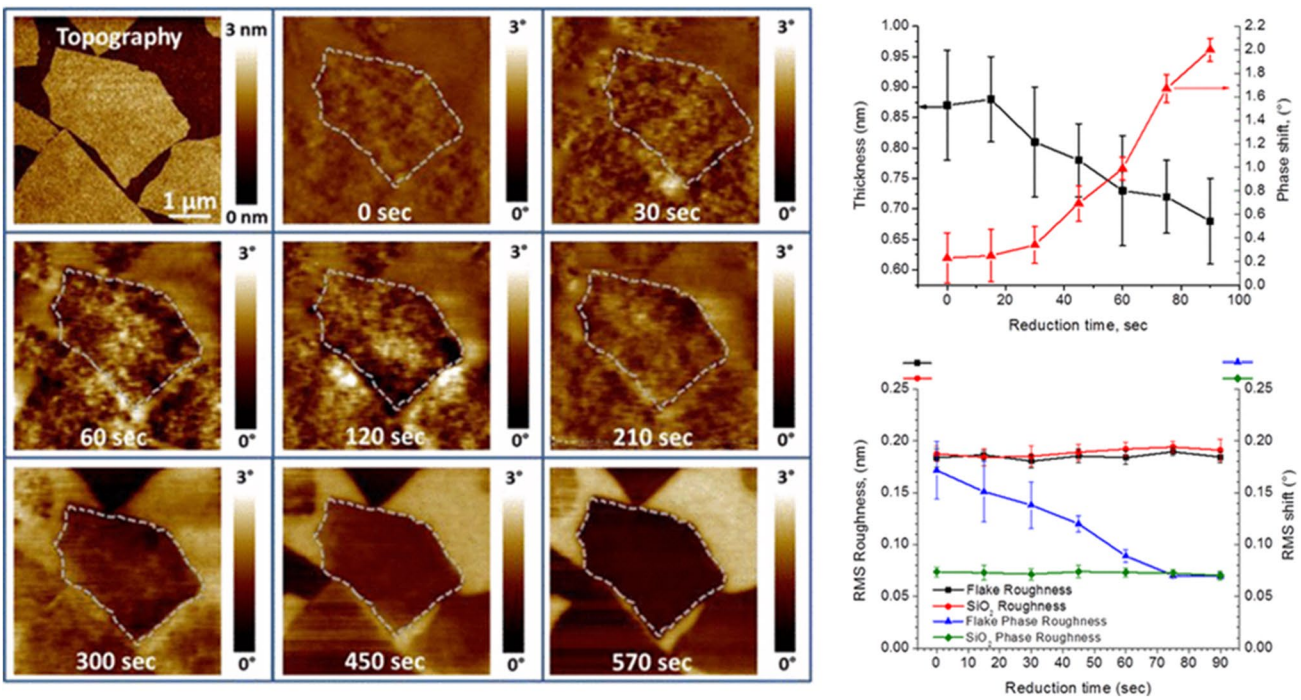

Figure 6. Topography and Electrostatic Force Microscopy (EFM) images of the same graphene oxide nanosheet during chemical reducing reaction under hydrazyne (left); nanosheet thinning and chemical phase increase (top). Corresponding plots of thickness and roughness versus reduction time (in seconds). Adapted with permission from Ref. 80.

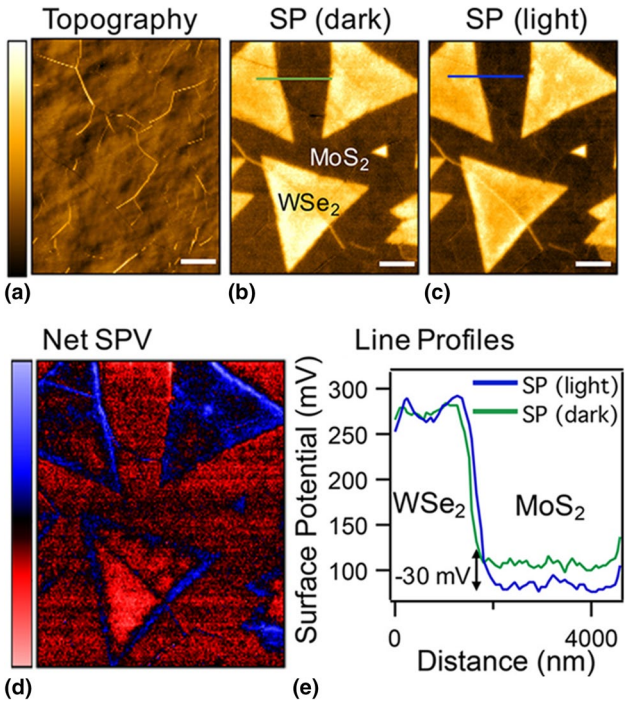

Figure 7. KPFM maps of WSe_2-MoS_2 heterostructures. (a) Topography image of the heterostructure. (b) Surface potential (SP) map taken under no illumination and (c) under illumination by a 401.5 nm laser diode. (d) Net surface photovoltage (SPV). (e) Line profiles of surface potential corresponding to (b) and (c). All scale bars 2 μm. Reprinted with permission from Ref. 85.

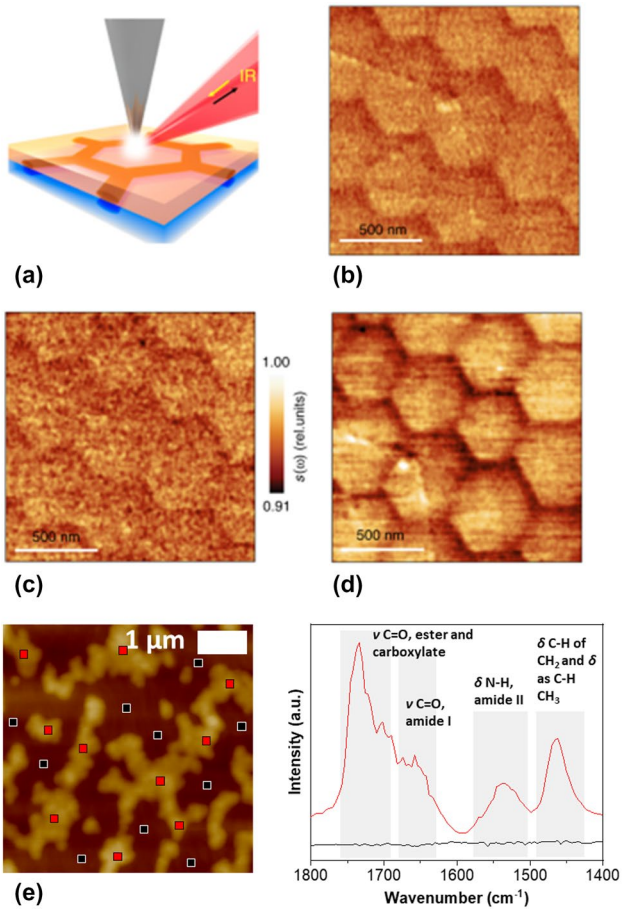

Figure 8. (a) Schematic of nano-IR probing method. Nano-IR images of hexagonal boron nitride (hBN) domains at varying frequencies, (b) 1344, (c) 1320, and (d) 1368 cm^{-1}. AFM topography image and AFM-IR spectra from thin films based on thermo-responsive polymers. Adapted with permission from Refs. 88, 90.

relevant for polymer-grafted 2D stacks, the heterogeneous surface chemistry of thermo-responsive ionic polymer monolayers was revealed by using high-resolution nano-IR mapping [Fig. 8(e)].[90]

As known, machine learning (ML) analysis methods have been utilized in materials science to accelerate materials discovery, automate materials characterization techniques, analyze big data sets, predict materials properties, and ultimately establish structure–property relationships.[91–93] It is worth to note that ML approaches can further enhance comprehensive understanding of heterostructure properties and in particularly, advances in imaging techniques. For example, ML methods were used to discover hidden patterns and establish correlations between Raman and photoluminescence spectra of 2D MoS_2 films.[94] Recently, the utilization of artificial intelligence (AI) driven scanning probe microscopy was explored to minimize the required datasets needed to reconstruct 3D piezoresistive probe microscopy images, and accelerate and guide dataset collection by determining possible measurement points of interest using Bayesian uncertainty.[95] In another study, ML models were used in conjunction with AFM and friction force microscopy (FFM) to correlate graphene layers with frictional properties.[95]

In conclusion, novel and diverse 2D heterostructures are promising functional nanomaterials for a variety of different emerging technologies, due to their unique properties including high ionic conductivity, enhanced mechanical stability, complementary transport pathways, and interfacial chemical endurance. We suggest that *in-situ* growth methods of metal oxides on MXenes via SI-ATRP will facilitate enhanced compositional, interlayer and interfacial chemistry control and versatility, leading to improved conduction, organization and operational stability for an array of prospective critical materials applications. The advances in fine surface and interfacial synthesis and nanoscale-resolution properties characterization approaches discussed here are the key to design and advance novel heterostructures with high architectural control and versatile interfacial chemistry for further advances of diverse applications in energy storage, energy transport, electronic communication, multifunctional sensors, and electronic protection.

Acknowledgments

The authors thank Prof. S. Kang, Prof. M. Kim, and Prof. Y. Gogotsi for important discussions and recent collaboration in this field. Financial support for this research is provided by the Air Force Office for Scientific Research grant

FA9550-20-1-0305, the Air Force Research Laboratory via UTC contract 165852-18F5828-19-16-C1 and the National Science Foundation DMR 2001968 and CHE 2200366 Awards.

Funding

Funding was provided by AFRL, AFOSR, and NSF Division of Materials Research and Division of Chemistry.

Declarations

Conflict of interest

The authors have no conflict of interest to declare.

References

1. C. Tan, X. Cao, X.J. Wu, Q. He, J. Yang, X. Zhang, J. Chen, W. Zhao, S. Han, G.H. Nam, M. Sindoro, H. Zhang, Recent advances in ultrathin two-dimensional nanomaterials. Chem. Rev. **117**, 6225–6331 (2017). https://doi.org/10.1021/acs.chemrev.6b00558
2. Y. Yang, C. Han, B. Jiang, J. Iocozzia, C. He, D. Shi, T. Jiang, Z. Lin, Graphene-based materials with tailored nanostructures for energy conversion and storage. Mater. Sci. Eng. R Rep. **102**, 1–72 (2016). https://doi.org/10.1016/j.mser.2015.12.003
3. A.K. Geim, K.S. Novoselov, The rise of graphene. Nature **6**, 183–191 (2007). https://doi.org/10.1038/nmat1849
4. A. VahidMohammadi, J. Rosen, Y. Gogotsi, The world of two-dimensional carbides and nitrides (MXenes). Science **372**, 1581 (2021). https://doi.org/10.1126/science.abf1581
5. N.F. Chiu, C.D. Yang, C.C. Chen, T.L. Lin, C.T. Kuo, Chapter 4—Functionalization of graphene and graphene oxide for plasmonic and biosensing applications, in *Graphene bioelectronics*. (Elsevier, USA, 2018)
6. K. Adstedt, M.L. Buxton, L.C. Henderson, D.J. Hayne, D. Nepal, Y. Gogotsi, V.V. Tsukruk, 2D graphene oxide and MXene nanosheets at carbon fiber surfaces. Carbon **203**, 161–171 (2023). https://doi.org/10.1016/j.carbon.2022.11.028
7. Y. Shi, W. Zhou, A.Y. Lu, W. Fang, Y.H. Lee, A.L. Hsu, S.M. Kim, K.K. Kim, H.Y. Yang, L.J. Li, Van der Waals epitaxy of MoS_2 layers using graphene as growth templates. Nano Lett. **12**, 2784–2791 (2012). https://doi.org/10.1021/nl204562j
8. A. Geim, I. Grigorieva, Van der Waals heterostructures. Nature **499**, 419–425 (2013). https://doi.org/10.1038/nature12385
9. S.H. Choi, S.J. Yun, Y.S. Won, C.S. Oh, S.M. Kim, K.K. Kim, Y.H. Lee, Large-scale synthesis of graphene and other 2D materials towards industrialization. Nat. Commun. **13**, 1484 (2022). https://doi.org/10.1038/s41467-022-29182-y
10. J. Mei, T. Liao, Z. Sun, Two-dimensional metal oxide nanosheets for rechargeable batteries. J. Energy Chem **27**, 117–127 (2018). https://doi.org/10.1016/j.jechem.2017.10.012
11. J. Mei, T. Liao, L. Kou, Z. Sun, Two-dimensional metal oxide nanomaterials for next-generation rechargeable batteries. Adv. Mater. **29**, 1700176 (2017). https://doi.org/10.1002/adma.201700176
12. B.K. Peters, K.X. Rodriguez, S.H. Reisberg, S.B. Beil, D.P. Hickey, Y. Kawamata, M. Collins, J. Starr, L.R. Chen, S. Udyavara, K. Klunder, T.J. Gorey, S.L. Anderson, M. Neurock, S.D. Minteer, P.S. Baran, Scalable and safe synthetic organic electroreduction inspired by Li-ion battery chemistry. Science **363**(6429), 838–845 (2019). https://doi.org/10.1126/science.aav5606
13. C. Xia, C.Y. Kwok, L.F.A. Nazar, High-energy-density lithium-oxygen battery based on a reversible four-electron conversion to lithium oxide. Science **361**(6404), 777–781 (2018). https://doi.org/10.1126/science.aas9343
14. S. Yu, R.D. Schmidt, R. Garcia-Mendez, E. Herbert, N.J. Dudney, J.B. Wolfenstine, J. Sakamoto, D.J. Siegel, Elastic properties of the solid electrolyte $Li_7La_3Zr_2O_{12}$ (LLZO). Chem. Mater. **28**, 197–206 (2015). https://doi.org/10.1021/acs.chemmater.5b03854
15. M.R. Lukatskaya, B. Dunn, Y. Gogotsi, Multidimensional materials and device architectures for future hybrid energy storage. Nat. Comm. **7**, 1 (2016). https://doi.org/10.1038/ncomms12647
16. M. Naguib, Y. Gogotsi, Synthesis of two-dimensional materials by selective extraction. Acc. Chem. Res. **48**, 128–135 (2015). https://doi.org/10.1021/ar500346b
17. M.T. Greiner, L. Chai, M.G. Helander, W.M. Tang, Z.H. Lu, Transition metal oxide work functions: the influence of cation oxidation state and oxygen vacancies. Adv. Funct. Mater. **22**, 4557–4568 (2012). https://doi.org/10.1002/adfm.201200615
18. M. Naguib, O. Mashtalir, J. Carle, J. Presser, J. Lu, L. Hultman, Y. Gogotsi, M.W. Barsoum, Two-dimensional transition metal carbides. ACS Nano **6**, 1322–2133 (2012). https://doi.org/10.1021/nn204153h
19. M. Naguib, M. Kurtoglu, V. Presser, J. Lu, J. Niu, M. Heon, L. Hultman, Y. Gogotsi, M.W. Barsoum, Two-dimensional nanocrystals produced by exfoliation of Ti_3AlC_2. Adv. Mater. **23**, 4248–4253 (2011). https://doi.org/10.1002/adma.201102306
20. B. Anasori, M.R. Lukatskaya, Y. Gogotsi, 2D metal carbides and nitrides (MXenes) for energy storage. Nat. Rev. Mater. **2**, 16098 (2017). https://doi.org/10.1038/natrevmats.2016.98
21. M. Naguib, V.N. Mochalin, M.W. Barsoum, Y. Gogotsi, 25th Anniversary article: MXenes: a new family of two-dimensional materials. Adv. Mater. **26**, 992–1005 (2014). https://doi.org/10.1002/adma.201304138
22. Y. Sun, D. Chen, Z. Liang, Two-dimensional MXenes for energy storage and conversion applications. Mater. Today Energy **5**, 22–36 (2017). https://doi.org/10.1016/j.mtener.2017.04.008
23. B. Ahmed, D.H. Anjum, Y. Gogotsi, H.N. Alshareef, Atomic layer deposition of SnO_2 on MXene for Li-ion battery anodes. Nano Energy **34**, 249–256 (2017). https://doi.org/10.1016/j.nanoen.2017.02.043
24. J. Azadmanjiri, V.K. Srivastava, P. Kumar, J. Wang, A. Yu, Graphene-supported 2D transition metal oxide heterostructures. J. Mater. Chem. A **6**, 13509–13537 (2018). https://doi.org/10.1039/C8TA03404D
25. M. Velicky, P.S. Toth, From two-dimensional materials to their heterostructures: an electrochemist's perspective. Appl. Mater. Today **8**, 68–103 (2017). https://doi.org/10.1016/j.apmt.2017.05.003
26. Y. Aierken, C. Sevik, O. Gulseren, F.M. Peeters, D. Cakir, MXenes/graphene heterostructures for Li battery applications: a first principles study. J. Mater. Chem. A. **6**, 2337–2345 (2018). https://doi.org/10.1039/C7TA09001C
27. Y. Xia, T.S. Mathis, M.Q. Zhao, B. Anasori, A. Dang, Z. Zhou, H. Cho, Y. Gogotsi, S. Yang, Thickness-independent capacitance of vertically aligned liquid-crystalline MXenes. Nature **557**, 409–412 (2018). https://doi.org/10.1038/s41586-018-0109-z
28. Y. Nagao, Proton-conductivity enhancement in polymer thin films. Langmuir **33**, 12547–12558 (2017). https://doi.org/10.1021/acs.langmuir.7b01484
29. C. Zhang, E. Staunton, Y.G. Andreev, P.G. Bruce, Raising the conductivity of crystalline polymer electrolytes by aliovalent doping. J. Am. Chem. Soc. **127**, 18305–18308 (2005). https://doi.org/10.1021/ja056129w
30. L.Y. Yang, D.X. Wei, M. Xu, Y.F. Yao, Q. Chen, Transferring lithium ions in nanochannels: a PEO/Li^+ solid polymer electrolyte design. Angew. Chem. Int. Ed. **53**, 3631–3635 (2014). https://doi.org/10.1002/anie.201307423
31. G. Zhang, Y.L. Hong, Y. Nishiyama, S. Bai, S. Kitagawa, S. Horike, Accumulation of glassy poly (ethylene oxide) anchored in a covalent organic framework as a solid-State Li^+ electrolyte. J. Am. Chem. Soc. **141**, 1227–1234 (2019). https://doi.org/10.1021/jacs.8b07670
32. C. Zhang, S. Gamble, D. Ainsworth, A.M. Slawin, Y.G. Andreev, P.G. Bruce, Alkali metal crystalline polymer electrolytes. Nat. Mater. **8**, 580–584 (2009). https://doi.org/10.1038/nmat2474
33. H. Dai, X. Zhao, H. Xu, J. Yang, J. Zhou, Q. Chen, G. Sun, Design of vertically aligned two-dimensional heterostructures of rigid $Ti_3C_2T_x$ MXene and pliable vanadium pentoxide for efficient lithium-ion storage. ACS Nano **16**, 5556–5565 (2022). https://doi.org/10.1021/acsnano.1c10212
34. J.R. Varcoe, P. Atanassov, D.R. Dekel, A.M. Herring, M.A. Hickner, P.A. Kohl, A.R. Kucernak, W.E. Mustain, K. Nijmeijer, K. Scott, Anion-exchange membranes in electrochemical energy systems. Energy Environ. Sci. **7**, 3135–3191 (2014). https://doi.org/10.1039/C4EE01303D

35. C. Liu, Z.G. Neale, G. Cao, Understanding electrochemical potentials of cathode materials in rechargeable batteries. Mater. Today **19**, 109–123 (2016). https://doi.org/10.1016/j.mattod.2015.10.009
36. S. Mogurampelly, O. Borodin, V. Ganesan, Computer simulations of ion transport in polymer electrolyte membranes. Annu. Rev. Chem. Biomol. Eng. **7**, 349–371 (2016). https://doi.org/10.1146/annurev-chembioeng-080615-034655
37. S. Morejudo, R. Zanón, S. Escolástico, I. Yuste-Tirados, H. Malerød-Fjeld, P. Vestre, W. Coors, A. Martínez, T. Norby, J. Serra, Direct conversion of methane to aromatics in a catalytic co-ionic membrane reactor. Science **353**, 563–566 (2016). https://doi.org/10.1126/science.aag0274
38. C.J. Yu, S.H. Choe, G.C. Ri, S.C. Kim, H.S. Ryo, Y.J. Kim, Ionic diffusion and electronic transport in eldfellite $Na_xFe(SO_4)_2$. Phys. Rev. Appl. **8**, 024029 (2017). https://doi.org/10.1103/PhysRevApplied.8.024029
39. E. Pomerantseva, Y. Gogotsi, Two-dimensional heterostructures for energy storage. Nat. Energy **2**, 17089 (2017). https://doi.org/10.1038/nenergy.2017.89
40. X. Wang, Q. Weng, Y. Yang, Y. Bandob, D. Golberg, Hybrid two-dimensional materials in rechargeable battery applications and their microscopic mechanisms. Chem. Soc. Rev. **45**, 4042–4073 (2016). https://doi.org/10.1039/c5cs00937e
41. S.T. Mahmud, M. Hasan, S. Bain, S.T. Rahman, M. Rhaman, M. Hossain, Multilayer MXene heterostructures and nanohybrids for multifunctional applications: a review. ACS Mater. Lett. **4**, 1174–1206 (2022). https://doi.org/10.1021/acsmaterialslett.2c00175
42. Y. Wang, J. Song, W.Y. Wong, Constructing 2D sandwich-like MOF/MXene heterostructures for durable and fast aqueous zinc-ion batteries. Angew. Chem. Int. Ed. **135**, e202218343 (2023). https://doi.org/10.1002/anie.202218343
43. K. Qian, Q. Zhou, S. Thaiboonrod, J. Fang, M. Miao, H. Wu, S. Cao, X. Feng, Highly thermally conductive Ti3C2Tx/h-BN hybrid films via coulombic assembly for electromagnetic interference shielding. J. Colloid Interf. Sci. **613**, 488–498 (2022). https://doi.org/10.1016/j.jcis.2022.01.060
44. R. Jerome, A.K. Sundramoorthy, Preparation of hexagonal boron nitride doped graphene film modified sensor for selective electrochemical detection of nicotine in tobacco sample. Anal. Chim. Acta **1132**, 110–120 (2020). https://doi.org/10.1016/j.aca.2020.07.060
45. X. Li, M. Zhang, Y. Hu, J. Xu, D. Sun, T. Hu, Z. Ni, Screen-printed electrochemical biosensor based on a ternary Co@MoS_2/rGO functionalized electrode for high-performance non-enzymatic glucose sensing. Biomed. Microdevices **22**, 17 (2020). https://doi.org/10.1007/s10544-020-0472-z
46. R. Sakthivel, M. Keerthi, R.J. Chung, J.H. He, Heterostructures of 2D materials and their applications in biosensing. Prog. Mater. Sci. **132**, 101024 (2023). https://doi.org/10.1016/j.pmatsci.2022.101024
47. N.C. Osti, M.W. Thompson, K.L. Van Aken, M. Alhabeb, M. Tyagi, J.-K. Keum, P.T. Cummings, Y. Gogotsi, E. Mamontov, Humidity exposure enhances microscopic mobility in a room-temperature ionic liquid in MXene. J. Phys. Chem. C **122**, 27561–27566 (2018). https://doi.org/10.1021/acs.jpcc.8b09677
48. K. Nasrin, V. Sudharshan, K. Subramani, M. Sathish, Insights into 2D/2D MXene heterostructures for improved synergy in structure toward next-generation supercapacitors: a review. Adv. Funct. Mater. **32**, 2110267 (2022). https://doi.org/10.1002/adfm.202110267
49. L. Wang, X. Zhang, Y. Xu, C. Li, W. Liu, S. Yi, K. Wang, X. Sun, Z.S. Wu, Y. Ma, Tetrabutylammonium-intercalated 1T-MoS_2 nanosheets with expanded interlayer spacing vertically coupled on 2D delaminated MXene for high-performance lithium-ion capacitors. Adv. Funct. Mater. **31**, 2104286 (2021). https://doi.org/10.1002/adfm.202104286
50. H. Xu, M. Li, S. Gong, F. Zhao, Y. Zhao, C. Li, J. Qi, Z. Wang, H. Wang, X. Fan, W. Peng, J. Liu, Constructing titanium carbide MXene/reduced graphene oxide superlattice heterostructure via electrostatic self-assembly for high-performance capacitive deionization. J. Colloid Interf. Sci. **624**, 223–241 (2022). https://doi.org/10.1016/j.jcis.2022.05.131
51. Z. Xing, J. Hu, M. Ma, H. Lin, Y. An, Z. Liu, Y. Zhang, J. Li, S. Yang, From one to two: In situ construction of an ultrathin 2D–2D closely bonded heterojunction from a single-phase monolayer nanosheet. J. Am. Chem. Soc. **141**, 19715–19727 (2019). https://doi.org/10.1021/jacs.9b08651
52. K. Chen, Y. Guan, Y. Cong, H. Zhu, K. Li, J. Wu, Z. Dong, G. Yuan, Q. Zhang, X. Li, Vertically pillared V2CTx/Ti3C2Tx flexible films for high-performance supercapacitors. J. Alloys Comp. **906**, 164302 (2022). https://doi.org/10.1016/j.jallcom.2022.164302
53. C. Jiang, V.V. Tsukruk, Freestanding nanostructures via layer-by-layer assembly. Adv. Mater. **18**, 829–840 (2006). https://doi.org/10.1002/adma.200502444
54. H. An, T. Habib, S. Shah, H. Gao, A. Patel, I. Echols, X. Zhao, M. Radovic, M.J. Green, J.L. Lutkenhaus, Water sorption in MXene/polyelectrolyte multilayers for ultrafast humidity sensing. ACS Appl. Nano Mater. **2**, 948–955 (2019). https://doi.org/10.1021/acsanm.8b02265
55. I.J. Echols, J. Yun, H. Cao, R.M. Thakur, A. Sarmah, Z. Tan, R. Littleton, M. Radovic, M.J. Green, J.L. Lutkenhaus, Conformal layer-by-layer assembly of $Ti_3C_2T_z$ MXene-only thin films for optoelectronics and energy storage. Chem. Mater. **34**, 4884–4895 (2022). https://doi.org/10.1021/acs.chemmater.1c04394
56. J. Yun, I. Echols, P. Flouda, S. Wang, A. Easley, X. Zhao, Z. Tan, E. Prehn, G. Zi, M. Radovic, M.J. Green, J.L. Lutkenhaus, Layer-by-layer assembly of polyaniline nanofibers and MXene thin-film electrodes for electrochemical energy storage. ACS Appl. Mater. Interfaces **11**, 47929–47938 (2019). https://doi.org/10.1021/acsami.9b16692
57. Y. Li, J. Zhang, Q. Chen, X. Xia, M. Chen, Emerging of heterostructure materials in energy storage: a review. Adv. Mater. **33**, 2100855 (2021). https://doi.org/10.1002/adma.202100855
58. Y.X. Gan, A.H. Jayatissa, Z. Yu, X. Chen, M. Li, Hydrothermal synthesis of nanomaterials. J. Nanomater. **1**, 1–3 (2020). https://doi.org/10.1155/2020/8917013
59. W. Zheng, Z. Zhang, N. Liu, Q. Li, J. Sun, Heterolayered SnO_2/SnSe nanosheets for detection of NO_2 at room temperature. ACS Appl. Nano Mater. **5**, 2436–2444 (2022). https://doi.org/10.1021/acsanm.1c04100
60. E. Xu, Y. Zhang, H. Wang, Z. Zhu, J. Quan, Y. Chang, P. Li, D. Yu, Y. Jiang, Ultrafast kinetics net electrode assembled via MoSe2/MXene heterojunction for high-performance sodium-ion batteries. Chem. Eng. J. **385**, 123839 (2020). https://doi.org/10.1016/j.cej.2019.123839
61. J. Li, B. Rui, W. Wei, P. Nie, L. Chang, Z. Le, M. Liu, H. Wang, L. Wang, X. Zhang, Nanosheets assembled layered MoS2/MXene as high performance anode materials for potassium ion batteries. J. Power Sources **449**, 227481 (2020). https://doi.org/10.1016/j.jpowsour.2019.227481
62. L. Yan, G. Chen, S. Sarker, S. Richins, H. Wang, W. Xu, X. Rui, H. Luo, Ultrafine Nb_2O_5 nanocrystal coating on reduced graphene oxide as anode material for high performance sodium ion battery. ACS Appl. Mater. Interfaces **8**, 22213–22219 (2016). https://doi.org/10.1021/acsami.6b06516
63. J. Cheng, B. Wang, H.L. Xin, G. Yang, H. Cai, F. Nie, H. Huang, Self-assembled V_2O_5 nanosheets/reduced graphene oxide hierarchical nanocomposite as a high-performance cathode material for lithium-ion batteries. J. Mater. Chem. A **1**, 10814–10820 (2013). https://doi.org/10.1039/C3TA12066J
64. M. Boota, B. Anasori, C. Voigt, M.Q. Zhao, M.W. Barsoum, Y. Gogotsi, Pseudocapacitive electrodes produced by oxidant-free polymerization of pyrrole between the layers of 2D titanium carbide (MXene). Adv. Mater. **28**, 1517–1522 (2016). https://doi.org/10.1002/adma.201504705
65. J. Fu, J. Yun, S. Wu, L. Li, L. Yu, K.H. Kim, Architecturally robust graphene-encapsulated MXene Ti2CT x@ Polyaniline composite for high-performance pouch-type asymmetric supercapacitor. ACS Appl. Mater. Interfaces **10**, 34212–34221 (2018). https://doi.org/10.1021/acsami.8b10195
66. A. VahidMohammadi, J. Moncada, H. Chen, E. Kayali, J. Orangi, C.A. Carrero, M. Beidaghi, Thick and freestanding MXene/PANI pseudocapacitive electrodes with ultrahigh specific capacitance. J. Mater. Chem. A **6**, 22123–22133 (2018). https://doi.org/10.1039/C8TA05807E
67. N. Binti Hamzan, C.Y.B. Ng, R. Sadri, M.K. Lee, L.J. Chang, M. Tripathi, A. Dalton, B.T. Goh, Controlled physical properties and growth mechanism of manganese silicide nanorods. J. Alloys Compd. **851**, 156693 (2021). https://doi.org/10.1016/j.jallcom.2020.156693
68. Y. Jiang, R. Wang, X. Li, Z. Ma, L. Li, J. Su, Y. Yan, X. Song, C. Xia, Photovoltaic field-effect photodiodes based on double van der Waals heterojunctions. ACS Nano **15**, 14295–14304 (2021). https://doi.org/10.1021/acsnano.1c02830
69. M. Sathiya, A. Prakash, K. Ramesha, J.M. Tarascon, A.K. Shukla, V_2O_5-anchored carbon nanotubes for enhanced electrochemical energy storage. J. Am. Chem. Soc. **133**, 16291–16299 (2011). https://doi.org/10.1021/ja207285b

70. Y. Liu, J. Wang, M. Zhang, H. Li, Z. Lin, Polymer-ligated nanocrystals enabled by nonlinear block copolymer nanoreactors: synthesis, properties and applications. ACS Nano **14**, 12491–12521 (2020). https://doi.org/10.1021/acsnano.0c06936
71. K. Matyjaszewski, P.J. Miller, N. Shukla, B. Immaraporn, A. Gelman, B.B. Luokala, T.M. Siclovan, G. Kickelbick, T. Vallant, H. Hoffmann, T. Pakula, Polymers at interfaces: using atom transfer radical polymerization in the controlled growth of homopolymers and block copolymers from silicon surfaces in the absence of untethered sacrificial initiator. Macromolecules **32**, 8716–8724 (1999). https://doi.org/10.1021/ma991146p
72. Y. Qiu, Z. Wang, A.C. Owens, I. Kulaots, Y. Chen, A.B. Kane, R.H. Hurt, Antioxidant chemistry of graphene-based materials and its role in oxidation protection technology. Nanoscale **6**, 11744–11755 (2014). https://doi.org/10.1039/C4NR03275F
73. T. Habib, X. Zhao, S.A. Shah, Y. Chen, W. Sun, H. An, J.L. Lutkenhaus, M. Radovic, M.J. Green, Oxidation stability of Ti3C2Tx MXene nanosheets in solvents and composite films. npj 2D Mater. Appl. **3**, 1–8 (2019). https://doi.org/10.1038/s41699-019-0089-3
74. M.-Q. Zhao, M. Torelli, C.E. Ren, M. Ghidiu, Z. Ling, B. Anasori, M.W. Barsoum, Y. Gogotsi, 2D titanium carbide and transition metal oxides hybrid electrodes for Li-ion storage. Nano Energy **30**, 603–613 (2016). https://doi.org/10.1016/j.nanoen.2016.10.062
75. M.C. Krecker, D. Bukharina, C.B. Hatter, Y. Gogotsi, V.V. Tsukruk, Bioencapsulated MXene flakes for enhanced stability and composite precursors. Adv. Funct. Mater. **30**, 2004554 (2020). https://doi.org/10.1002/adfm.202004554
76. G. Decher, Fuzzy nanoassemblies: toward layered polymeric pulticomposites. Science **277**, 1232 (1997). https://doi.org/10.1126/science.277.5330.1232
77. A.P.R. Johnston, C. Cortez, A.S. Angelatos, F. Caruso, Layer-by-layer engineered capsules and their applications. Curr. Opin. Colloid Interface Sci. **11**, 203–209 (2006). https://doi.org/10.1016/j.cocis.2006.05.001
78. K. Hu, D.D. Kulkarni, I. Choi, V.V. Tsukruk, Graphene-polymer nanocomposites for structural and functional applications. Prog. Polym. Sci. **39**, 1934–1972 (2014). https://doi.org/10.1016/j.progpolymsci.2014.03.001
79. D.D. Kulkarni, S. Kim, M. Chyasnavichyus, K. Hu, A.G. Fedorov, V.V. Tsukruk, Chemical reduction of individual graphene oxide sheets as revealed by electrostatic force microscopy. J. Am. Chem. Soc. **136**, 6546–6549 (2014). https://doi.org/10.1021/ja5005416
80. L. Sun, N. Sun, Y. Liu, C. Jiang, Anisotropic frictional properties between $Ti_3C_2T_x$ MXene/SiO_2 layer-dependent heterojunctions. J. Sci. Adv. Mater. Dev **6**, 488–493 (2021). https://doi.org/10.1016/j.jsamd.2021.05.006
81. W. Yang, F. Zhou, B. Xu, Y. Hong, X. Ding, J. Sun, L.Z. Liu, C. Zheng, J. Deng, The interfacial adhesion of contacting pairs in van der Waals materials. Appl. Surf. Sci. **598**, 153739 (2022). https://doi.org/10.1016/j.apsusc.2022.153739
82. H. Rokni, W. Lu, Direct measurements of interfacial adhesion in 2D materials and van der Waals heterostructures in ambient air. Nat. Commun. **11**, 5607 (2020). https://doi.org/10.1038/s41467-020-19411-7
83. S. Luo, T. Alkhidir, S. Mohamed, S. Answer, B. Li, J. Fu, K. Liao, V. Chan, Investigation of interfacial interaction of graphene oxide and $Ti_3C_2T_x$ (MXene) via atomic force microscopy. Appl. Surf. Sci. **609**, 155303 (2023). https://doi.org/10.1016/j.apsusc.2022.155303
84. M.J. Shearer, M.Y. Li, L.J. Li, S. Jin, R. Hamers, Nanoscale surface photovoltage mapping of 2D materials and heterostructures by illuminated kelvin probe force microscopy. J. Phys. Chem. C **122**, 13564–13571 (2018). https://doi.org/10.1021/acs.jpcc.7b12579
85. Y. Wang, Y. Gong, L. Yang, Z. Xiong, Z. Lv, X. Xing, Y. Zhou, B. Zhang, C. Su, Q. Liao, S.T. Han, MXene-ZnO memristor for multimodal in-sensor computing. Adv. Fun. Mater. **31**, 2100144 (2021). https://doi.org/10.1002/adfm.202100144
86. J.E. Heckler, G.R. Neher, F. Mehmood, D.B. Lioi, R. Pachter, R. Vaia, W.J. Kennedy, D. Nepal, Surface functionalization of $Ti_3C_2T_x$ MXene nanosheets with catechols: implication for colloidal processing. Langmuir **37**, 5447–5456 (2021). https://doi.org/10.1021/acs.langmuir.0c03078
87. G.X. Ni, H. Wang, B.Y. Jiang, L.X. Chen, Y. Du, Z.Y. Sun, M.D. Goldflam, A.J. Frenzel, X.M. Xie, M.M. Fogler, D.N. Basov, Soliton superlattices in twisted hexagonal boron nitride. Nat. Commun. **10**, 4360 (2019). https://doi.org/10.1038/s41467-019-12327-x
88. F. Hu, M. Kim, Y. Zhang, Y. Luan, K.M. Ho, Y. Shi, C.Z. Wang, X. Wang, Z. Fei, Tailored plasmons in pentacene/graphene heterostructures with interlayer electron transfer. Nano Lett. **19**, 6058–6064 (2019). https://doi.org/10.1021/acs.nanolett.9b01945
89. P. Flouda, A.V. Stryutsky, M.L. Buxton, K.M. Adstedt, D. Bukharina, V.V. Shevchenko, V.V. Tsukruk, Reconfiguration of Langmuir monolayers of thermo-responsive branched ionic polymers with LCST transition. Langmuir **38**, 12070–12081 (2022). https://doi.org/10.1021/acs.langmuir.2c01940
90. E.S. Muckley, R. Vasudevan, B.G. Sumpter, R.C. Advincula, I.N. Ivanov, Machine intelligence-centered system for automated characterization of functional materials and interfaces. ACS Appl. Mater. Interfaces **15**, 2329–2340 (2023). https://doi.org/10.1021/acsami.2c16088
91. N. Andrejevic, J. Andrejevic, B.A. Bernevig, N. Regnault, F. Han, G. Fabbris, T. Nguyen, N.C. Drucker, C.H. Rycroft, M. Li, Machine-learning spectral indicators of topology. Adv. Mater. **34**, 2204113 (2022). https://doi.org/10.1002/adma.202204113
92. Z. Si, D. Zhou, J. Yang, X. Lin, Review: 2D material property characterizations by machine-learning-assisted microscopies. Appl. Phys. A **129**, 248 (2023). https://doi.org/10.1007/s00339-023-06543-y
93. A.Y. Lu, L.G.P. Martins, P.C. Shen, Z. Chen, J.H. Park, M. Xue, J. Han, N. Mao, M.H. Chiu, T. Palacios, V. Tung, J. Kong, Unraveling the correlation between Raman and photoluminescence in monolayer MoS_2 through machine-learning models. Adv. Mater. **34**, 2202911 (2022). https://doi.org/10.1002/adma.202202911
94. M. Ziatdinov, D. Kim, S. Neumayer, R.K. Vasudevan, L. Collins, S. Jesse, M. Ahmadi, S.V. Kalinin, Imaging mechanism for hyperspectral scanning probe microscopy via Gaussian process modelling. NPJ Comput. Mater. **6**, 21 (2020). https://doi.org/10.1038/s41524-020-0289-6
95. F. Cellini, F. Lavini, C. Berger, W. de Heer, E. Riedo, Layer dependence of graphene-diamene phase transition in epitaxial and exfoliated few-layer graphene using machine learning. 2D Materials **6**, 035043 (2019). https://doi.org/10.1088/2053-1583/ab1b9f